Iranian Journal of Chemical Engineering

Journal Homepage: www.ijche.com

pISSN: 1735-5397
eISSN: 2008-2355

Regular Article

Numerical Study of the Fluid Flow and Erosion-Corrosion in an Industrial Valve

K.H. Hanon, E. Ebrahimi *

Department of Mechanical Engineering, Kermanshah Branch, Islamic Azad University, Kermanshah, Iran.

ARTICLE INFO

Article history:
Received: 2022-12-01
Accepted: 2023-06-12
Available online: 2023-07-11

Keywords:
Erosion,
CFD,
Butterfly valve,
Cavitation,
Modeling

ABSTRACT

The purpose of this research is the CFD modeling of the fluid flow inside an industrial valve in order to discover the areas with high shear stress and to determine the effect of hydrodynamic on the erosion rate. CFD results are compared with the existing experimental data in a valid reference and the model is verified with high accuracy. The impact of the pressure at inlet and the disc angle on the erosion is investigated. By increasing the inlet pressure, the maximum velocity, turbulence intensity, wall shear stress and particle erosion increased. However, the wall shear stress, turbulence intensity, and particle erosion are clearly reduced as the disc angle decreased. When the disc angle is less than 50^o, the changes in dependent parameters are small. Reducing the disc angle or increasing the inlet pressure led to an increase in cavitation. Therefore, to prevent the erosion of the butterfly valve, it is necessary to increase the disc angle or reduce the pressure at inlet. The erosion of the butterfly valve significantly occurred at the front and rear of the disc. Depending on the disc angle, the shear stress of wall for the modified configuration is 10 to 80 times lower than that for the original butterfly valve. Therefore, it can be stated that the modified geometry can reduce the wall shear stress and consequently the erosive effect for all of the disc angles of the studied butterfly valve.

DOI: 10.22034/ijche.2023.375055.1466 URL: https://www.ijche.com/article_174787.html

1. Introduction

Erosion-corrosion in pipelines and industrial valves during operations is categorized into two main parts of the chemical corrosion and the erosion caused by the fluid flow, cavitation and solid particles. The first case that is the chemical corrosion inside this equipment generated by corrosive chemicals in oil and gas. Sulfur compounds, carbon dioxide (CO_2), oxygen (O_2) and water can be mentioned from among the main chemical

*Corresponding author: e.ebrahimi57@gmail.com (E. Ebrahimi)

compounds in oil and gas that cause the internal corrosion. The hydrogen sulfide gas alone does not cause corrosion, but when it is combined with water droplets, it forms acid and causes corrosion, and when it is combined with CO_2 and O_2 gases, corrosion becomes much more severe. In their study, Stack and Abdulrahman [1], investigated the combined impacts of erosion and collision on carbon steel over a a wide range of potentials, velocities and impact angles , velocities, and impact angles in three environments, including crude oil, tank water, and a mixture of both suspensions. The results show that the contribution to corrosion enhanced by increasing the water content in the tank. In another study, Stack and Abdulrahman [2] found that the erosion of solid particles in the oil/water mud was a significant technical field. In these situations, it is essential to distinguish between exposure to sand, water, and oil. Rashidi et al. [3] assessed the corrosive behavior of active MDEA (methyldiethanolamine) suspensions in the CO_2 bulk elimination at an ammonia plant. The impacts of hydrodynamics and the velocity distribution on the corrosion properties of the air-cooled amine heat exchanger (ACHE) were then evaluated by the author through the experimental research and CFD simulation [4]. Recently, Bo et al [5] reported an analysis based on the theory of erosion caused by the solid particle in actual industrial butterfly valves. The research conducted by Valeh-Sheyda [6] tries to evaluate the impacts of erosion-corrosion to check the E-C interactivities inside the industrial valve and both sides of the valve including two pairs of diffuser-elbows. The visual observations from the photographs of the damaged areas of carbon steel were used to validate the CFD results.

In a study, Li et al. [7] investigated the corrosion of the X65 pipe steel in the CO_2-saturated oil-free water with various electrochemical measurements and Computational Fluid Dynamic (CFD). It has been found that in both oil-free suspensions and oil-water emulsions, the mass transport of corrosive species such as H_2 and H_2CO_3 has been shown to dominate the cathodic process during the steel corrosion. Increasing the flow rate speeds up the mass transfer and corrosion. The existence of oil in the liquid reduces the corrosion of the steel and enhances the oil content. The purpose of the study by Meriem-Benziane et al. [8] is to investigate the use of the emulsion flow (oil-water) in steel pipe-lines. The CFD modeling was used to investigate flow, pressure, and velocity gradients across pipe walls. The excistence of Crude oil and water emulsions are remarkable in the petroleum and chemical industries. Naphthenic acid (NA) is found in crude oil and causes corrosion in pipelines. One of the purposes of this investigation is to compute the velocity profile based on the rheological models such as the Herschel-Bulkley model and the Ostwald model. In the study performed by Redondo et al. [9] it was simulated the hydrocarbon pipe erosion-corrosion with a CFD-based method. This technique provides a very accurate 3D representation of the flow mode, phase distribution, and contact area for the pipe, allowing the accurate calculations of erosion and corrosion velocities and distributions on the pipeline surface. McLaury [10] proposed generalized erosion prediction procedures including flow simulation, particle tracking, and erosion simulation. This is now usually known as the CFD-based erosion prediction. In a study done by Jia et al. [11] a new test device has been developed to investigation the erosion and corrosion properties of 90° steel elbows in a three-phase gas-liquid-solid flow. Experimental and simulation results show that the strongest erosion and corrosion regions of the elbow happen at the axial bending angles of 20-50° and radial bending angles of -45° to +45°. At the bottom of the elbow and on the surface of the outer wall near the exit, the synergistic effect of erosion and corrosion accelerates pipeline wear, while the opposite phenomenon is at the elbow position with a shear angle of 50-70°.

Liu et al. [12] investigated the isolation valve installed in the circulating water treatment system "CWF". The simulation of a water reactor at a plant was done in combination with multiphase flow, cavitation, and discrete phase models to simulate erosion. The results show that the butterfly valve erosion happens primarily on the front and back of the disc. The numerical analysis of erosion situations improves the reliability of the butterfly valve.

In the study of Khadem-Hosseini et al. [13], the causes of the failure of the nickel aluminum bronze butterfly valve used in the seawater desalination unit in a refinery plant were investigated. Different analyzes such as SEM, EXD and EDS, and the chemical analysis were used to check the results. The effect of the opening of the butterfly valve on the fluid behavior and finally on the failure was simulated by the (CFD) numerical method.

Zhu et al. [14] investigated the deformation and flow erosion rate caused by the needle valve flow by the CFD modeling coupled with the discrete phase model. An acceptable agreement between the predicted and actual data was obtained. The effect of different parameters on the distribution of the gas-particle flow field and the degree of deformation and the erosion of the needle valve core were recorded. Their results show that among all the parameters, the valve tip has the greatest effect on deformation and erosion, and the flow field, deformation and erosion of the valve are all sensitive to changes in inlet conditions, structural changes, and changes in fluid properties.

Therefore, according to above reviews, in order to reduce the erosion of industrial valves used in oil and gas industries, the CFD modeling of the fluid flow to determine the area under erosion is necessary.

The two main reasons that cause the erosion of butterfly valves are cavitation and the particle erosion, which are numerically investigated in this research. Indeed, in this study it has been tried to consider and predict the erosion areas for the geometrical system including a pipeline and a butterfly valve. By predicting the erosive areas, a new idea is presented by modifying the geometry of the upstream and downstream of the butterfly valve to reduce the erosion. To validate the numerical data, the CFD results are compared to the experimental results in a valid reference based on the flow coefficient.

2. Numerical section

Butterfly valves are widely used in many cases due to their easy operation. However, according to the environmental conditions, they are exposed to erosion. These kinds of equipment are commonly used in the low pressure drop, shut down, fill/drain and bypass systems as well as for the flow and pressure control. Unlike other types of valves such as ball valves, this type of valves always has a disk in the flow, causing a pressure drop. The researchers obtained useful results by examining the characteristics of the flow and its effect on the butterfly valve. One of the results is that there is a possibility of cavitation occurring at different fluid velocities when applying butterfly valves in controls that are not completely open or closed. The velocity of the fluid flow along the pipe with a large cross-sectional area increases by passing over the valve seat, and as a result, the dynamic pressure increases and the static pressure decreases. The pressure drop across the valve seat under the vapor pressure creates bubbles at a sufficiently high liquid rate. The static pressure downstream of the valve is usually greater than the vapor pressure and creates energy in a small space that bursts the bubbles and creates pressures of thousands of psi. Studies show that opening the butterfly valve 20-40% provides the basis for cavitation [15]. In addition to these mechanical aspects, various electrochemical parameters also play roles [16-18]. The cavitation damage is amplified by the synergistic effect of the mechanical attack. The butterfly valve erosion has always been the focus of engineers and researchers [19] and is one of the leading causes of the butterfly valve failure, causing lots of economic losses each year. The two main causes of the butterfly valve erosion are cavity erosion [20] and particle erosion [21], that are investigated in this study. Since it is very rare to consider cavity erosion and particle erosion simultaneously in numerical analyzes in literatures, up to now, there is no relevant reference for investigating both erosions simultaneously, so; in this research it has been tried to investigate this issue and predict the erosion areas for the pipeline and butterfly valve.

2.1. Geometry, specifications and dimensions of the studied pipeline and butterfly valve

As mentioned, in this research, no experimental work has been done but the CFD modeling of the erosion process due to the fluid flow in a butterfly valve (Figure 1) has been investigated.

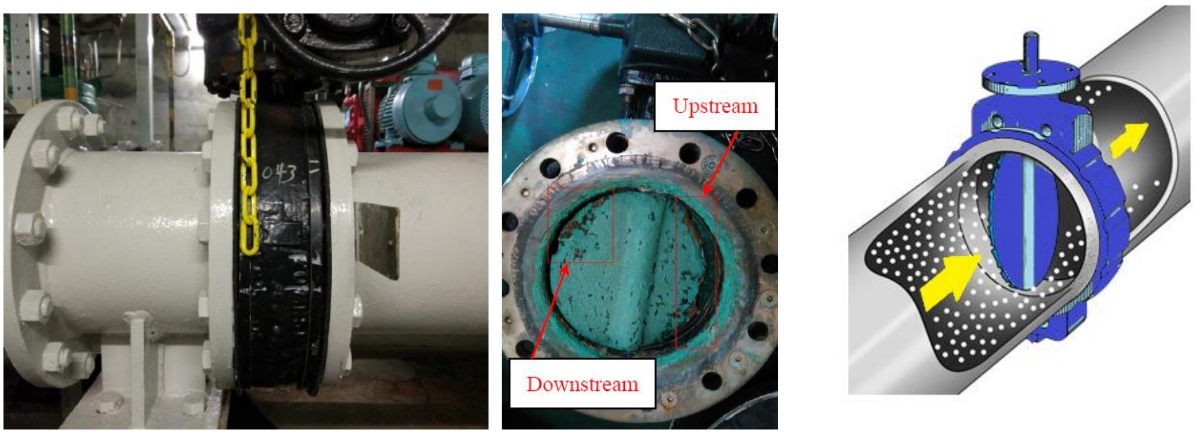

(a) (b)

Figure 1. (a) Real photo of the industrial butterfly valve [12], and (b) schematic of the pipeline and the butterfly valve.

In order to confirm the simulation results, one of the studied geometries has been compared with the results of a numerical work available in a valid article and confirmed [12]. To create the geometry for modeling, the butterfly valve was drawn in its original size in the Gambit software. Figure 2 shows the dimensions and schematic of the butterfly valve.

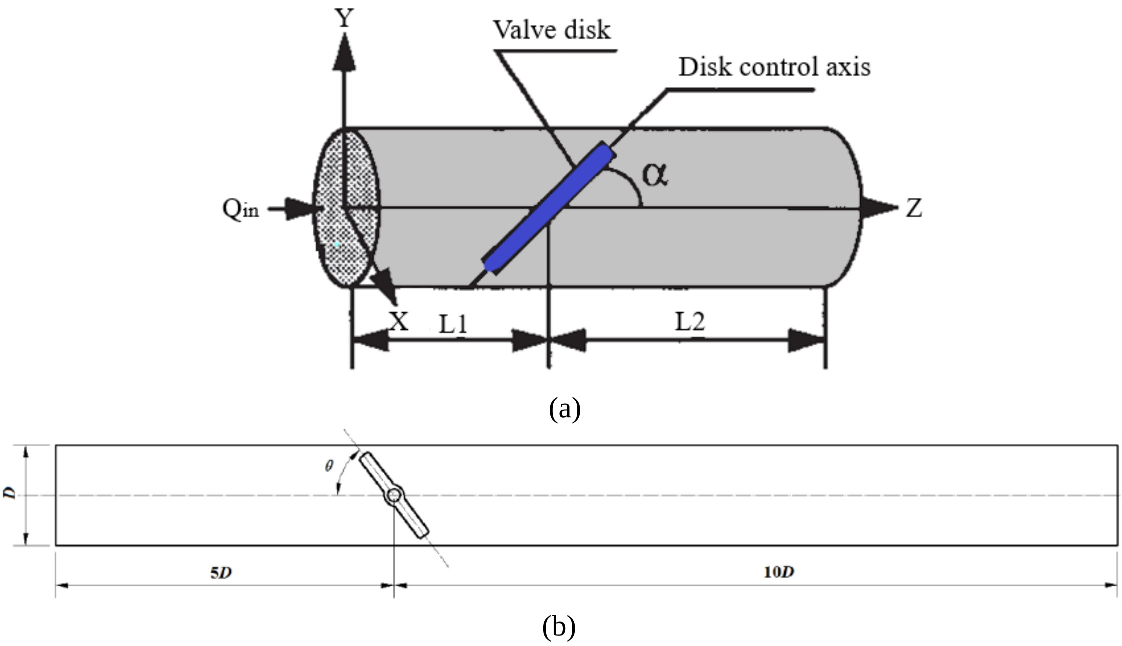

Figure 2. (a) Three-dimensional schematic, and (b) two-dimensional schematic of the pipeline and butterfly valve computational domain [12].

In the investigated geometry, the fluid flows in a pipe with a circular cross-section and the disc inside the butterfly valve is a flat circular plate. The diameter of the pipe is 200 mm. The angle of the disc varies from 0 to 90^o, which is measured from the horizontal position. V is the input velocity, which is variable in the Z direction. The thickness of the disc is 0.005 m [22].

To perform the CFD simulation, the first step is to create the system geometry in the Gambit software and meshing it. For this purpose, the butterfly valve and its upstream and downstream pipe-lines were created with exactly the same real dimensions. In order to do meshing, the geometric shape was divided into small control volumes. It is clear that the more the number of networks and the smaller the sizes of the meshes, the slower the calculation process and running time in the Fluent software. By examining and analyzing other researches, it is clear that the high level of turbulence near the pipe wall downstream of the butterfly valve is the key parameter that leads to the actual erosion in pipelines and the butterfly valve. The optimization of the flow field could be attained by improving the upstream and downstream structure of the butterfly disc. To modify the original butterfly valve, a bunch of blades placed on a semicircle are alternately placed upstream and downstream of it. To make the downstream blades, first a cylinder with a height of 10 mm and a radius of 100 mm is drawn in the x direction, and then a circle with the same length but the radius of 85 mm is subtracted from it to make a ring in the form of a rim. Then, cubic structures with the thickness of 0.01 m are subtracted from it. The improved structure on the both sides of the butterfly disc is shown in Figure 3. In fact, the new geometry proposed in this research is similar to the work of Liu et al. [12], but with the difference that in order to reduce the erosion caused by the fluid flow and wear, redundant parts are installed on the downstream and upstream of the butterfly valve.

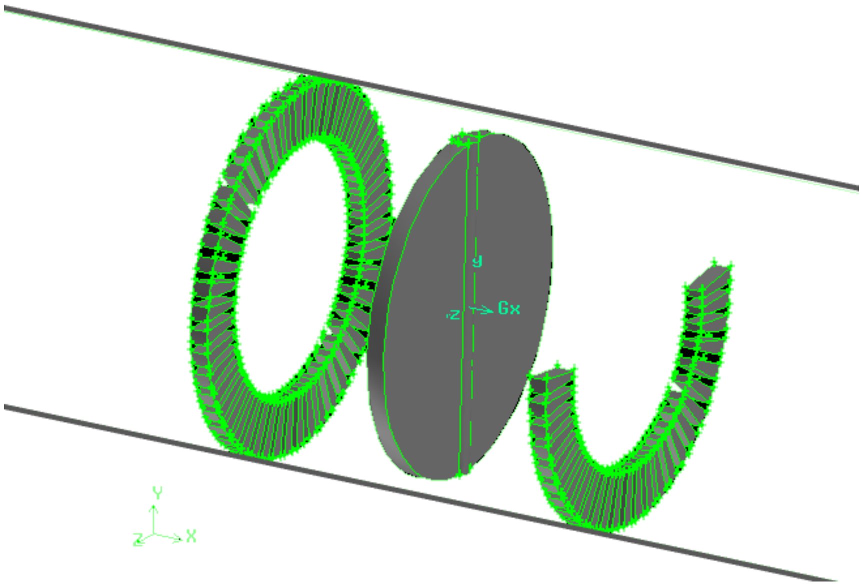

Figure 3. Redundant parts and the improved structure on the both sides of the butterfly disc.

2.2. Definition of materials, the determination of boundary conditions and meshing

The temperature of the inlet fluid was 27 °C and the mass component of the particles was 0.1% and their diameters were 500 µm. The saturated vapor pressure was also considered equal to 3.5×10^{-3} MPa. The boundary situations defined for this issue are the inlet velocity boundary for the flow inlet downstream, the outlet pressure for the outlet flow upstream of the butterfly valve, and the wall boundary condition for the pipe wall. The details of the boundary conditions are presented in Table 1.

Table 1

Boundary conditions applied to the investigated system.

Boundary name	**Boundary condition**
inlet	Velocity inlet
outlet	Pressure outlet
Butterfly valve wall	Wall
Tube wall	Wall

To consider the effect of different factors, changes in the inlet pressure and disc angle are the important factors. At the outlet, the pressure is set to 0.1 MPa. The CFD model was constructed at various disc angles, including 90 °, 70 °, 50 °, 30 °, and 10°, to examine the impacts of various disc angles individually. All solid walls, such as pipe walls and valve disk walls, have non-slip boundary conditions and the simulation model takes fluid gravity into account. Triangular meshes with the size of 0.01 m have been used for meshing the inlet and outlet plates of the pipeline, and hybrid meshes with the size of 0.01 m have been used for meshing the total volume. The velocity and pressure gradient around the disc change greatly, so the mesh size inside the disc is set to be less (0.005 m) compared to the same in other areas. Meshed geometries can be seen in Figure 4.

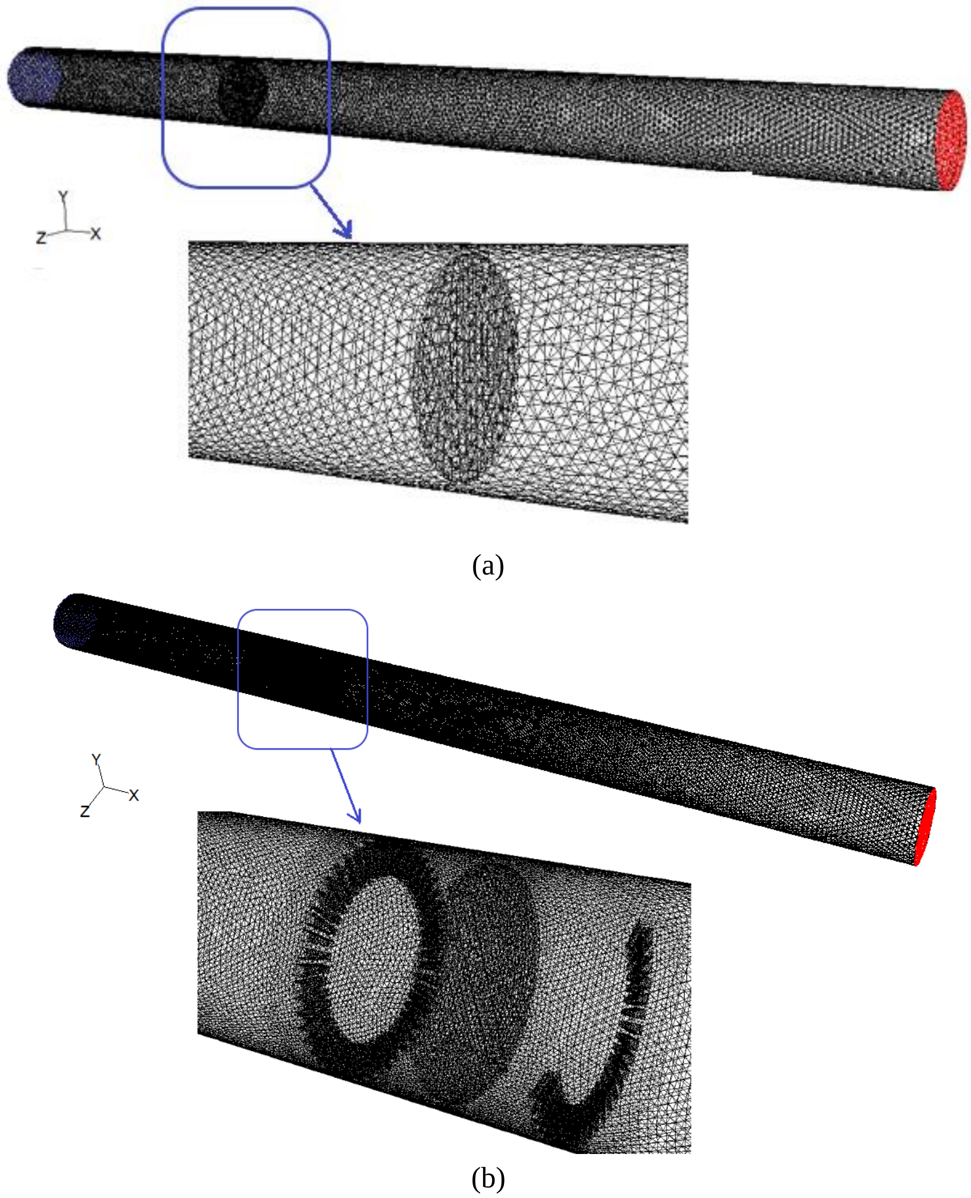

Figure 4. Meshed geometries investigated in this research, the (a) butterfly valve with a 90° disc - the pipeline proposed by Liu et al. [12], and (b) butterfly valve with 90° disc – the pipeline and attachments installed on the upstream and downstream.

2.3. Solution strategy and independence from meshes

For the CFD modeling, the SIMPLE algorithm was used for pressure-velocity coupling, and in order to discretize the pressure, the PRESTO method was used, and for the momentum the QUICK method was used. Calculations are considered under the steady-state condition. A mesh independence test was performed to ensure numerical predictions with the minimal levels of the mesh discretization influence. The selection of the numerical mesh was based on the discretization of the mesh with few control volumes, which showed the same behavior similar to that of the purest mesh, to avoid excessive computational processing costs and to ensure the minimization of the effect of the numerical discretization on the simulation results.

2.4. Numerical simulation Continuity equation:

The modeling of the desired systems includes the steady-state solution of the Navier-Stokes equations, which are expressed as follows for different quantities of φ [12]:

$$\frac{\partial(\rho_m)}{\partial t}+\nabla.(\rho_m \vec{v}_m)=0 \quad (1)$$

$$\rho_m=\sum_{i=1}^{k}\alpha_i\rho_i \quad (2)$$

ρ_m is the mixture density and α is the volume component of each phase.

Momentum equation:

The equation of momentum for the system under investigation is written as follows:

$$\frac{\partial(\rho_m \vec{v}_m)}{\partial t}+\nabla.(\rho_m \vec{v}_m \vec{v}_m)= \quad (3)$$
$$-\nabla p+\nabla.(\mu_m\left(\nabla\vec{v}_m+\nabla.\vec{v}_m^{\,T}\right))$$
$$+\rho_m\bar{g}+\vec{F}+\nabla(\sum_{i=1}^{k}\alpha_i\rho_i\vec{v}_{dr,i}\vec{v}_{dr,i})$$

Where ν is the fluid velocity and P is the static pressure. k is the number of phases, F is the volumetric force and μ is the viscosity of the mixture, which is expressed as follows:

$$\mu_m=\sum_{i=1}^{k}\alpha_i\mu_i \quad (4)$$

$$\vec{v}_{dr,i}=\vec{v}_i-v_m \quad (5)$$

Cavitation modeling:

In most of references, the three models of cavitation are proposed, which are Belamri , Schnerr and Sauer models.The second model proposed by Schnerr and Sauer has been widely used to predict cavitation. The equation of steam volume fraction is as follow [12]:

$$\frac{\partial(\alpha\rho_v)}{\partial t}+\nabla.(\alpha\rho_v\vec{v})=\frac{\rho_v\rho_l}{\rho}\frac{D\alpha}{Dt} \quad (6)$$

The net mass source expression is computed as:

$$R=\frac{\rho_v\rho_l}{\rho}\frac{d\alpha}{dt} \quad (7)$$

The relationship between the number of bubbles and the vapor volume fraction per the liquid volume is described as follows:

$$\alpha=\frac{4}{3}\frac{n_b\pi R^3_b}{1+n_b\frac{4}{3}\pi R^3_b} \quad (8)$$

Where R_b is the radius of the bubble, which can be expressed as follows:

$$R_b=(\frac{\alpha}{1-\alpha}\frac{3}{4\pi}\frac{1}{n_b})^{\frac{1}{3}} \quad (9)$$

Particle motion equations:

The inertia of a particle is equal to the force acting on the particle and can be reported as [12]:

$$\frac{d\vec{u}_p}{dt}=F_D(\vec{u}-\vec{u}_p)+\frac{g(\rho_p-\rho)}{\rho_p}+\vec{F} \quad (10)$$

Where $\vec{F}$ is the additional acceleration which can be written as:

$$F_D=C_{vm}\frac{\rho}{\rho_p}(\vec{u}_p\nabla\vec{u}-\frac{d\vec{u}_p}{dt}) \quad (11)$$

Where C_{vm} is known as the virtual mass coefficient with a defaulting amount of 0.5. Where $F_D(\vec{u}-\vec{u}_p)$ is the drag force per the unit mass of the particle and is computed as:

$$F_D=\frac{18\mu}{\rho_p d_p^{\,2}}\frac{C_D\,\mathrm{Re}}{24} \quad (12)$$

Here, u is the fluid phase velocity, particle velocity, μ represents the molecular viscosity of the fluid, ρ is the fluid density, ρ_p represents the particle density, and d_p represents the particle diameter. Re represents the relative Reynolds number, which is defined as:

$$\mathrm{Re}=\frac{\rho_p d_p}{\mu}(\vec{u}-\vec{u}_p) \quad (13)$$

Due to the turbulent flow in the throttle, the discrete probability distribution model is employed to estimate the particles dispersion because of turbulence. The liquid velocity u of the path equation (Equation 10-13) can be indicated as follows:

$$u = \bar{u} + u' \tag{14}$$

Where $\bar{u}$ and u' are the average velocity of the fluid phase, and oscillating velocity respectively, and u' is computed as:

$$u' = \xi \sqrt{\bar{u}'^2} \tag{15}$$

Where ξ is a normally distributed random number.

Theory of the particle erosion:

The erosion caused by particles and accretion rates can be showed at wall boundaries. The erosion rate can be calculated as:

$$R_{erosion} = \sum_{p=1}^{N} \frac{m_p C(d_p) \mathrm{f}(\alpha) \mathrm{v}^{b(v)}}{A_{face}} \tag{16}$$

Where m_p represents the particle mass flow, C (d_p) represents the function of the diameter of particles, α represents the angle of the particle trajectory with the wall surface, f (α) represents the function of the impact angle, v represents the relative particle. $b_{(v)}$ represents the function of the relative velocity of the particle and A represents the area of the cell plane at the wall.

3. Results and discussion

Figure 5 indicates the velocity contour for both geometries under consideration. The particle erosion significantly happens at the front of the disc, which causes corrosion at the front of the disc. The contour for the geometry of Liu et al. [12] in Figure 5 (a) indicates that the amount of the fluid velocity near the valve is high and the vectors indicate the rotation of the fluid in this area. The erosion of the butterfly valve significantly happens at the front and rear of the disc at θ=90° when the velocity is high. There is more particle erosion on the upstream side of the valve disk and abrasive erosion appears on one side of the valve disk. In general, the wear of the butterfly valve happens significantly around the edge of the disc, and a small amount is also observed on the cylinder face of the disc. Figure 5 (b) shows the positive effect of the modified geometry on reducing the velocity and also the fluid circulation around the propeller valve, which confirms the reduction of the wear corrosion.

.

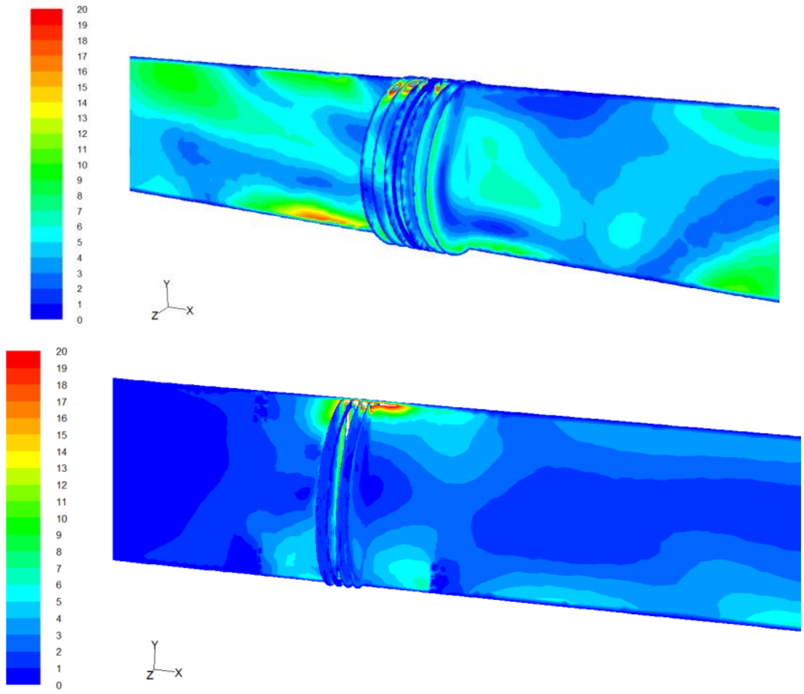

Figure 5. Velocity (m/s) contour for the disc angle of 90°.

To illustrate the flow specific of the butterfly valve, k_v (known as the flow coefficient) has been presented, which describes the pressure drop to in the flow velocity at a determined disc angle. The k_v can be defined as:

$$k_v = Q\sqrt{\frac{10\rho}{\rho_0 \Delta P}} \qquad (17)$$

Q is the flow rate in m^3/h, ρ and ρ_0 (1000 kg/m^3) are the fluid density and standard fluid density in kg/m^3 respectively, ΔP is the pressure drop in MPa. k_v can be estimated and computed with a numerical modeling in which the boundary conditions of the experiment are used. Figure 6 indicates the results of the k_v simulation that does not consider the impacts of cavitation and particles. The CFD results of the original butterfly valve are slightly higher than the experimental data and there is no clear trend of the modified geometry, but the CFD simulation results are in good agreement with the experimental data.

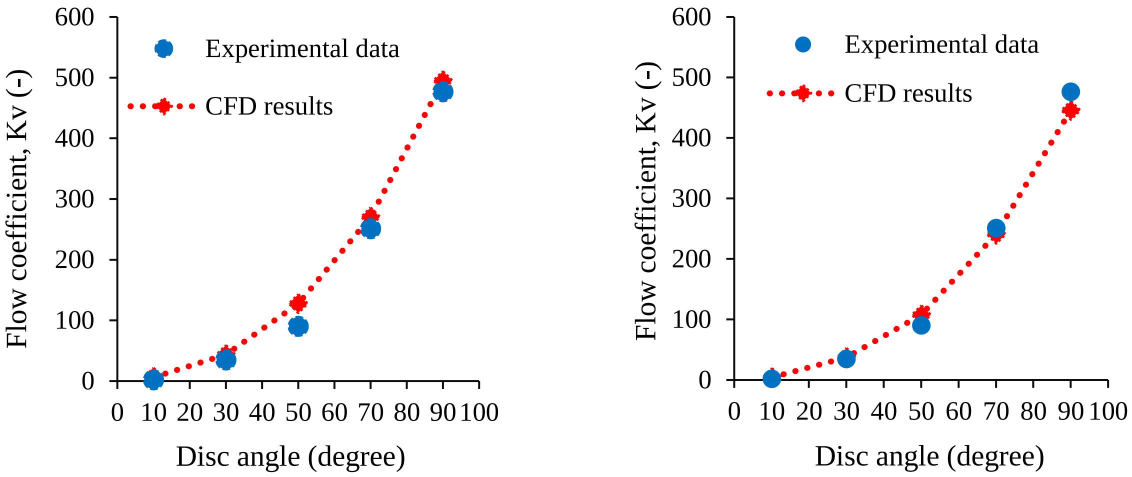

(a) (b)

Figure 6. Comparison of CFD data, when neglecting the impact of cavitation and particles, with experimental data [12] at different angles for disc, (a) the geometry proposed by Liu et al. [12], and (b) the modified geometry proposed in this research

Figure 7 shows the comparison of CFD results, when taking into account the effect of cavitation and particles, with experimental data [12] at different angles for disc. Figure 7 shows that if cavitation is considered, the agreement between the CFD data and the experimental data is better and the modeling is more accurate.

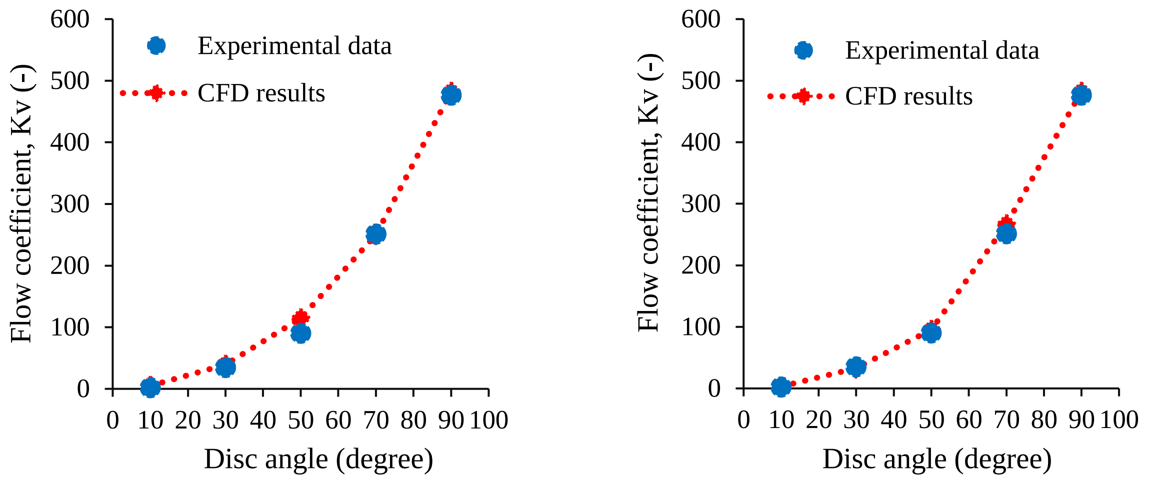

(a) (b)

Figure 7. Comparison of CFD results, when taking into account the effect of cavitation and particles, with experimental data [12] at different angles for disc, (a) the geometry proposed by Liu et al. [12], and (b) the modified geometry proposed in this research.

In this section, we computed numerical models of the coupling erosion, complex multi-phase models, cavitation, and discrete phases. The impacts of the pressure of the inlet and the disc angle are studied individually. The simulation is run by setting various amounts for the pressure of the inlet flow at each disc angle, but the other parameters are left at their defaults (the particle mass fraction=0.1%, outlet pressure=0.4 MPa, particle diameter=500μm). The simulation results including the maximum velocity at various pressures of inlet and various disk angles, the wall shear stress, turbulence intensity, and particle erosion rate are indicated in Figure 8 and Figure 9. The maximum speed first enhances and then slowly reduces with the reduction of the disc angle of the disk, as shown in Figure 8. However, the maximum speed clearly enhances by increasing the pressure of the inlet, when there is no change in the disc angle of the valve.

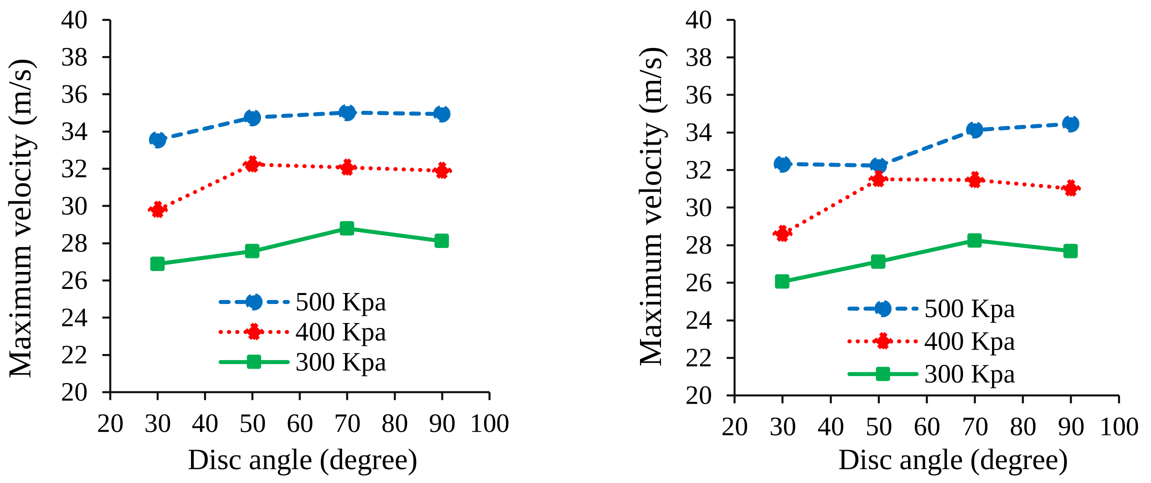

(a) (b)

Figure 8. Maximum velocity of the valve at several pressures at the inlet, (a) the geometry proposed by Liu et al. [12], and (b) the modified geometry proposed in this research.

The shear stress of the wall reduces immediately as the disc angle reduces and it enhances as the pressure of the inlet enhances. This is shown in Figure 9. The same tendency can be seen in the turbulent flow intensity and particle erosion indicated in Figures 9 and 10. Decreasing the disc angle to 50° tends to stabilize the magnitude of the wall shear stress.

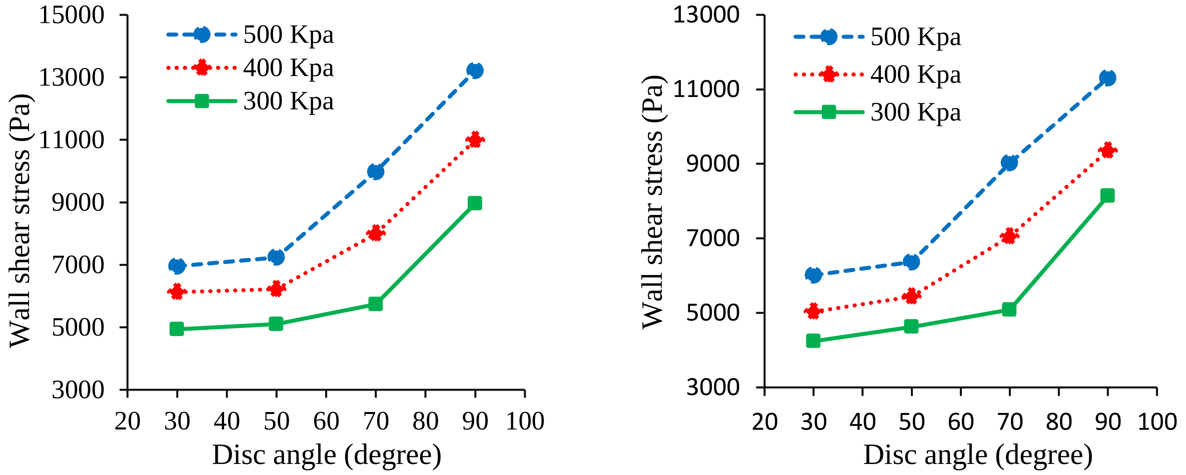

(a) (b)

Figure 9. Effect of the pressure at the inlet on the shear stress of the valve wall, (a) the geometry proposed by Liu et al. [12], and (b) the modified geometry proposed in this research.

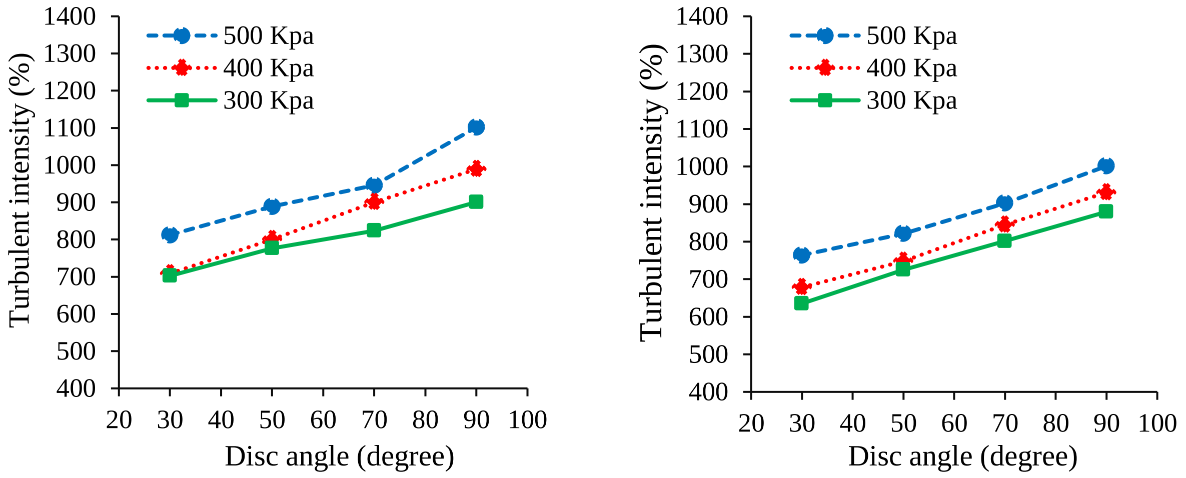

(a) (b)

Figure 10. Effect of the pressure at the inlet on the turbulence intensity of valve, (a) the geometry proposed by Liu et al. [12], (b) the modified geometry proposed in this research.

The erosion rate increases gradually with the decrease of the valve disc angle as shown in Figure 11. In addition, the erosion rate increases clearly with the increase of the inlet pressure, when the disc angle has no change. In fact, by applying the combined effect of cavitation and particle, the modeling results for the flow coefficient become more accurate and the validity of the model can be confirmed more.

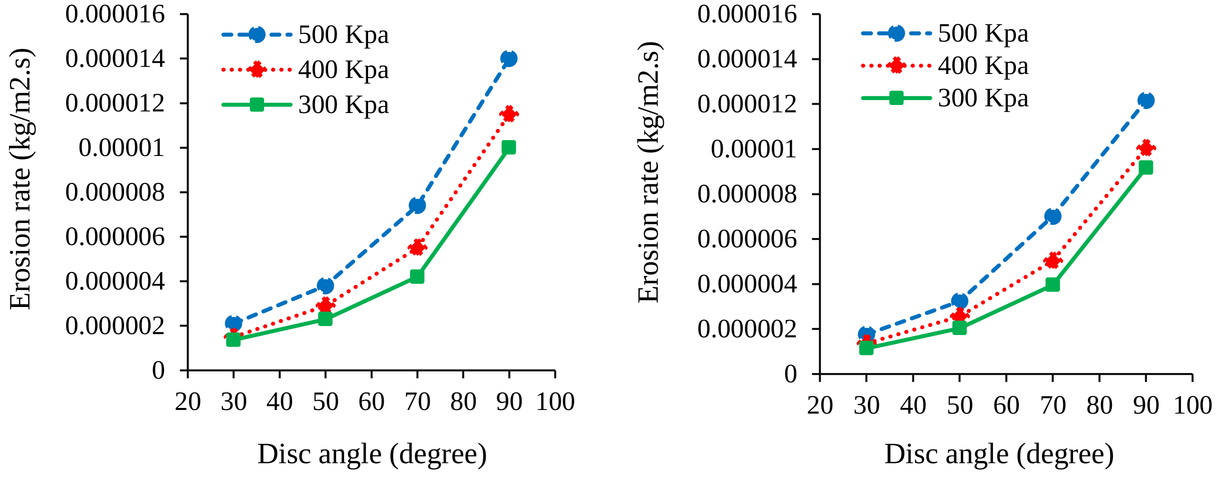

(a) (b)

Figure 11. Effect of the pressure at the inlet on the erosion rate of the valve, (a) the geometry proposed by Liu et al. [12], (b) the modified geometry proposed in this research

Figures 12, 13 and 14 show that the turbulent kinetic energy is high around the valve and for Liu et al. [12], its value is much higher than its amounts for the modified geometry. This proves the positive effect of the proposed appendage parts in decreasing the erosion of the butterfly valve and the pipeline close to it.
.

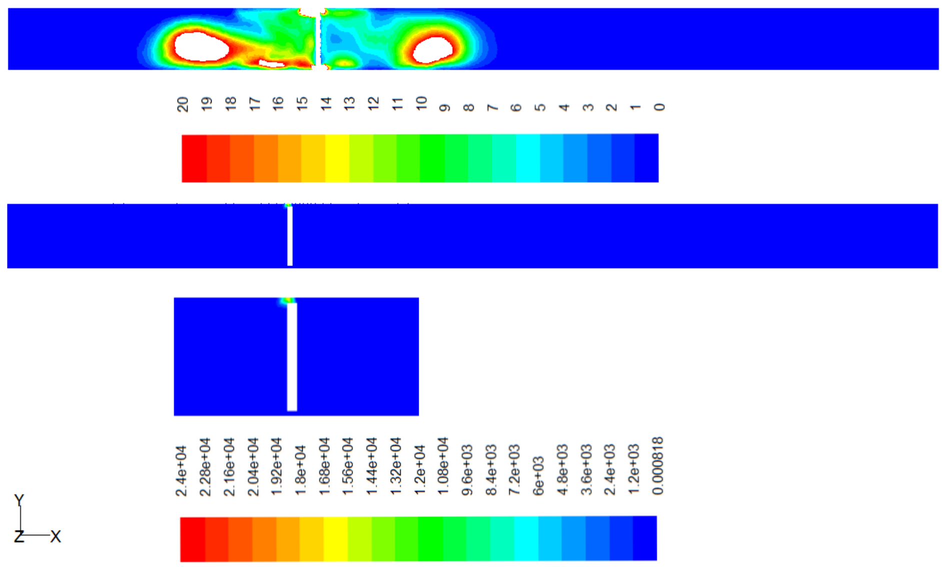

(a)

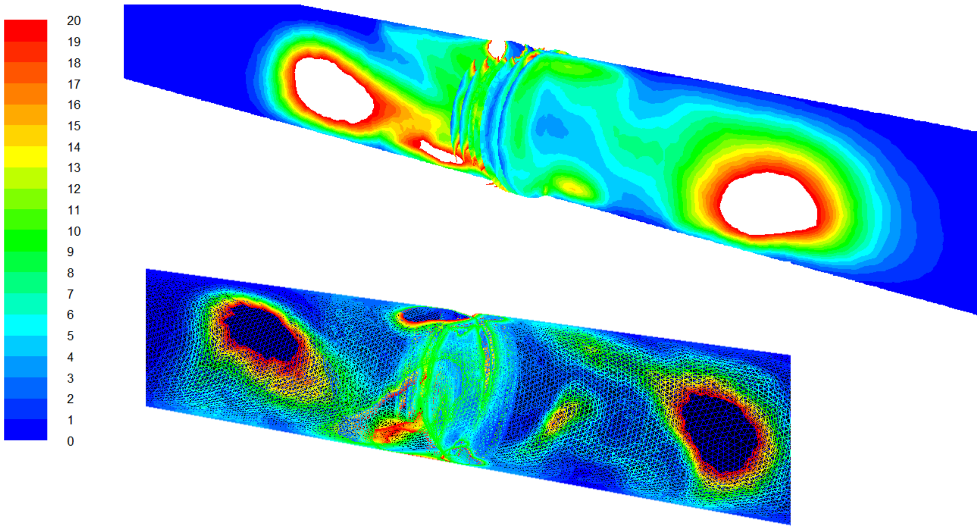

(b)

Figure 12. Turbulent kinetic energy contour (k) for a disk angle equal to 90 °(the pressure at the inlet of 500 kPa) for the geometry proposed by Liu et al [12], (a) 2-D, and (b) 3-D.

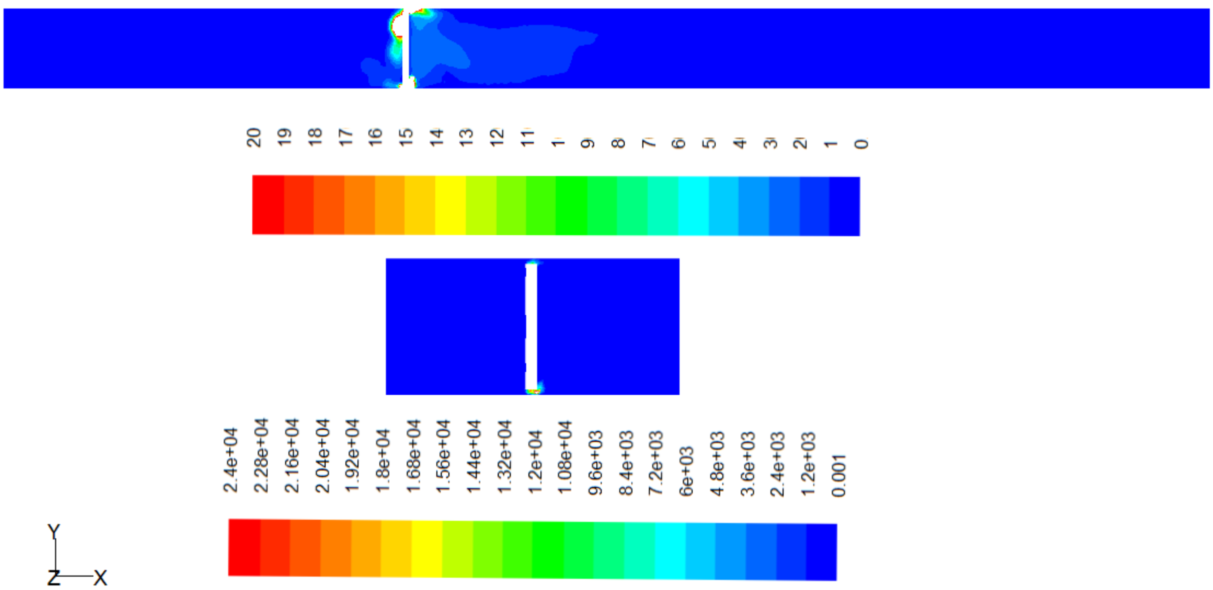

(a)

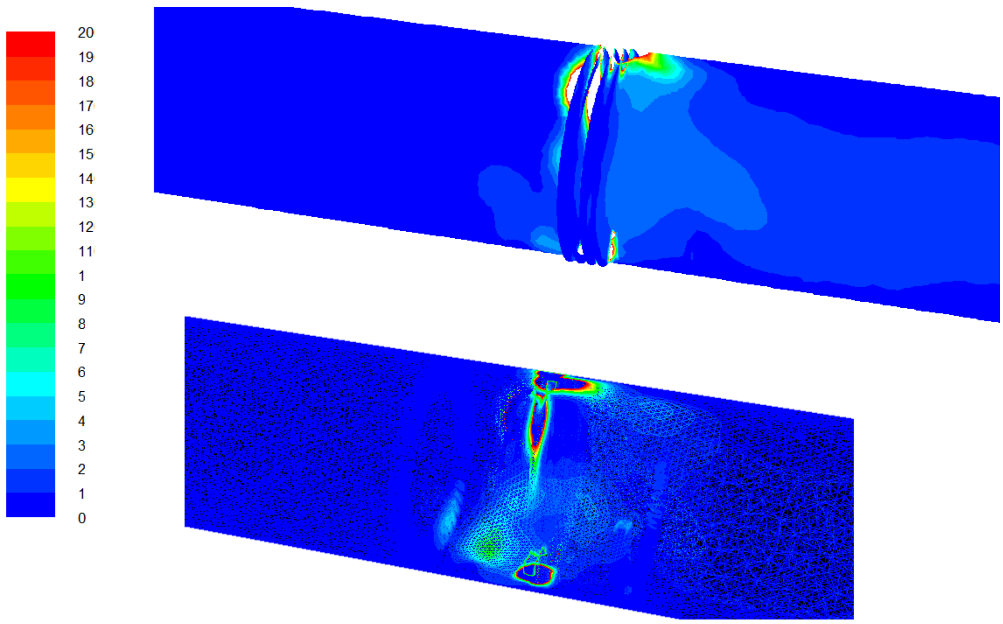

(b)

Figure 13. Contour of turbulent kinetic energy (k) for the disc angle equal to 90° (the pressure at the inlet of 500 kPa) for the modified geometry proposed in this study, (a) 2-D, and (b) 3-D.

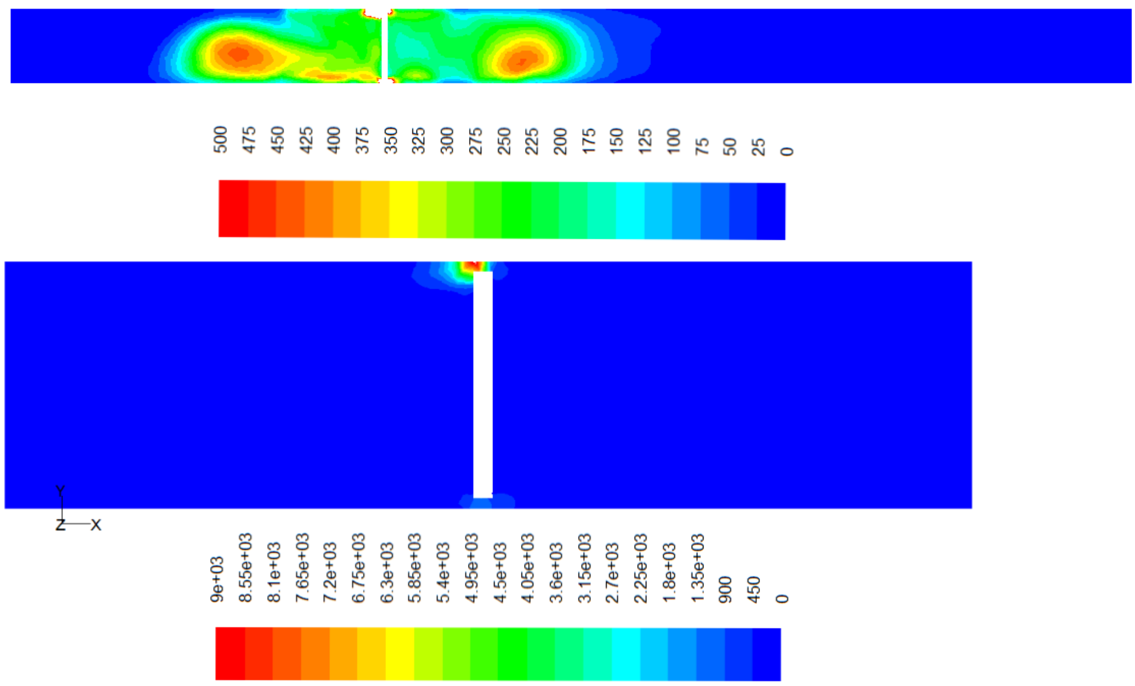

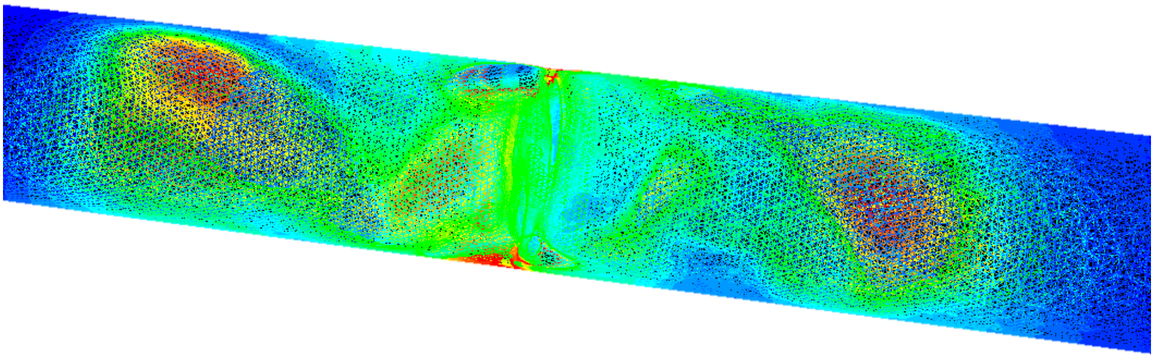

(a)

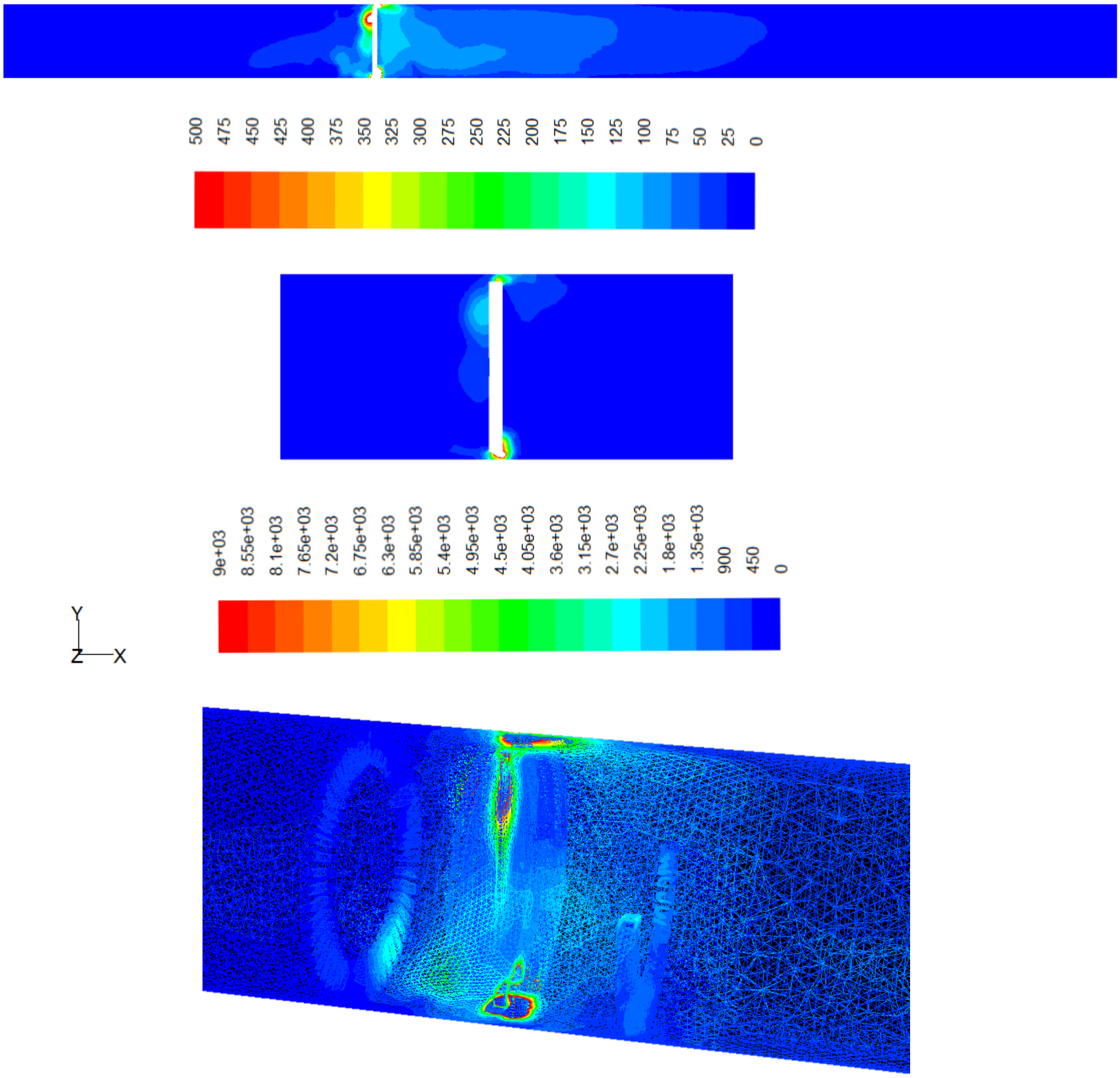

(b)

Figure 14. Turbulence intensity contour for the disc angle equal to 90° (the pressure at the inlet=500 kPa), (a) the geometry proposed by Liu et al. [12], and (b) the modified geometry proposed in this research

4. Conclusion

In this research, the CFD simulation of cavitation and discrete phase was conducted and analyzed to investigate the erosion of an industrial butterfly valve. The two main reasons that cause the erosion of butterfly valves are cavitation and the particle erosion, which were investigated. In this research we tried to consider this issue and predict erosion areas for the pipeline and butterfly valve. By predicting the erosive areas, a new idea was presented by modifying the geometry of the upstream and downstream of the butterfly valve to reduce the erosion. To validate the numerical data, the CFD results were compared with the existing experimental results for the flow coefficient in a valid reference. The results of the CFD model were verified with high accuracy. The effect of various parameters including the pressure of the inlet flow and the disc angle of the butterfly valve on its erosion was investigated. By increasing the inlet pressure of the flow, the maximum velocity, turbulence intensity, wall shear stress, and particle erosion increased. Nevertheless, the turbulence intensity, particle erosion and shear stress of the wall were obviously reduced by the reduction in the disc angle. Specifically, it can be stated that the limitation of the parameters is somewhat reduced when the disc angle of the valve is less than 50°. An increase in cavitation occurs as a result of reducing the disc angle or increasing the inlet pressure. The erosion of the front side of the disc is often caused by the particle erosion and the erosion in the rear part is strongly caused by the cavity erosion. Depending on the disc angle, the shear stress of the wall for the modified configuration was 10 to 80 times lower than the same for the original butterfly valve. In fact, the shear stress of the wall and the flow friction coefficient of the modified butterfly valve are very small compared to the original geometry for all disc angles. Therefore, it can be concluded that the modified configuration can reduce the shear stress of the wall and consequently the erosive corrosion for all the disc angles of the studied butterfly valve.

References

[1] M.M.Stack, G.H.Abdulrahman, Mapping erosion-corrosion of carbon steel in oil exploration conditions: Some new approaches to characterizing mechanisms and synergies, Tribology International 43, 7, 2010, 1268-1277.

[2] Stack, Margaret and Abdulrahman, Ghaith, Mapping erosion-corrosion of carbon steel in oil-water solutions : Effect of velocity and applied potential, Wear, 274-275. Pp. 401-413. ISSN 0043-1648 (https://doi.org/10.1016/j.wear.2011.10.008).

[3] H. Rashidi, P. Valeh-e-Sheyda, An insight on amine air-cooled heat exchanger tubes' corrosion in the bulk CO_2 removal plant, Int. J.Greenh. Gas Contr. 47 (2016) 101–109.

[4] P. Valeh-e-Sheyda, H. Rashidi, Inhibition of corrosion in amine air cooled heat exchanger: experimental and numerical study, Appl. Therm. Eng. 98 (2016) 1241–1250.

[5] L. Bo, Z. Jiangang, Q. Jianhua, Numerical study of solid particle erosion in butterfly valve, In: IOP Conference Series: Materials Science and Engineering, vol. 220, 2017, p. 012018, (1).

[6] Peyvand Valeh-e-Sheyda, Hamed Rashidi, Neda Azimi, Structural improvement of a control valve to prevent corrosion in acid gas treating plant pipeline: An experimental and computational analysis, International Journal of Pressure Vessels and Piping 165 (2018) 114-125.

[7] Qiang Li, Haitao Hu, Y.Frank Cheng, Corrosion of pipelines in CO_2-saturated

oil-water emulsion flow studied by electrochemical measurements and computational fluid dynamics modeling, Journal of Petroleum Science and Engineering. 147, (2016) 408-415.

[8] Madjid Meriem-Benziane, Hamou Zahloul, Ibrahim Gadi and Noureddine Boudouani, CFD modeling of the emulsions (oil-water) on pipelines corrosion, J Pet Environ Biotechnol 2013, 4:6, http://dx.doi.org/10.4172/2157-7463.S1.004.

[9] C. Redondo, M. Ch´avez–Moden, J. Manzanero, G. Rubioa, E. Valero, S. G´omez–Alvarez, A. Rivero–Jim´enez, CFD–based erosion and corrosion modeling in pipelines using a High–order discontinuous Galerkin multiphase solver. Wear 478–479, 15 (2021) 203882.

[10] B.S. McLaury, Predicting Solid Particle Erosion Resulting from Turbulent Fluctuations in Oilfield Geometries, 1997. Ph.D. thesis.

[11] Wenlong Jia, Yuanrui Zhang, Changjun Li, Peng Luo, Xiaoqin Song, Yuzhu Wang, Xinyi Hu, Experimental and numerical simulation of erosion-corrosion of 90◦ steel elbow in shale gas pipeline, Journal of Natural Gas Science and Engineering 89 (2021) 103871.

[12] Bo Liu, Jiangang Zhao, Jianhua Qian, Numerical analysis of cavitation erosion and particle erosion in butterfly valve, 2017. doi: 10.1016/j.engfailanal.2017.06.045.

[13] R. Khadem Hosseini, Sh. Yareiee, Failure analysis of a nickel aluminium bronze butterfly valve in a seawater line, Engineering Failure Analysis 129 (2021) 105686.

[14] Hongjun Zhu, Qian Pan, Wenli Zhang, Guang Feng, Xue L, CFD simulations of flow erosion and flow-induced deformation of needle valve: Impacts of operation, structure and fluid parameters, Nuclear Engineering and Design 273 (2014) 396–411.

[15] Bo-Suk Yang, Won-Woo Hwang, Myung-Han Ko, Soo-Jong Lee, Cavitation detection of butterfly valve using support vector machines, J. Sound Vib. 287 (1-2) (2005) 25–43, https://doi.org/10.1016/j.jsv.2004.10.033.

[16] E. Korkut, M. Atlar, On the importance of the effect of turbulence in cavitation inception tests of marine propellers, Proc. R. Soc. Lond. A 458 (2017) (2002) 29–48, https://doi.org/10.1098/rspa.2001.0852.

[17] A. Al-Hashem, W. Riad, The role of microstructure of nickel–aluminium–bronze alloy on its cavitation corrosion behavior in natural seawater, Mater. Charact. 48 (1) (2002) 37–41, https://doi.org/10.1016/S1044-5803(02)00196-1.

[18] A. Al-Hahem, P.G. Caceres, W.T. Riad, H.M. Shalaby, Cavitation corrosion behavior of cast nickel-aluminium bronze in seawater, Corrosion 51 (1995) 331–342, https://doi.org/10.5006/1.3293598.

[19] Z. Leutwyler, C. Dalton, A CFD of study of the flow field, resultant force, and aerodynamic torque on a symmetric disk butterfly valve in a compressible fluid, J Press Vess-T ASME 130(2) (2008) 1030-1036.

[20] P. Naseradinmousavi, C. Nataraj, Nonlinear mathematical modeling of butterfly valves driven by solenoid actuators, Appl Math Model 35(5) (2011) 2324-2335.

[21] G. Brett, M. Riveland, T. C. Jensen, et al., Cavitation from a butterfly valve: comparing 3D simulations to 3D X-ray computed tomography flow visualization, Proceedings of ASME-JSME-KSME Joint Fluids Engineering Conference (2011) 161-169.

[22] H. Zhu, Q. Pan, W. Zhang, et al., CFD simulations of flow erosion and flow-induced deformation of needle valve: Impacts of operation, structure and fluid parameters, Nucl Eng Des 273(1) (2014) 396-411.